Lawrence Berkeley Laboratory
UNIVERSITY OF CALIFORNIA

Materials & Molecular Research Division

Presented at the 7th International Conference on Noise in Physical Systems, Montpellier, France, May 16-20, 1983

CHAOS AND NOISE IN JOSEPHSON TUNNEL JUNCTIONS

J. Clarke, R.F. Miracky, J. Martinis, and R.H. Koch

May 1983

Prepared for the U.S. Department of Energy under Contract DE-AC03-76SF00098

DISCLAIMER

LBL-16127

CHAOS AND NOISE IN JOSEPHSON TUNNEL JUNCTIONS

John Clarke, Robert F. Miracky, and John Martinis

Department of Physics
University of California
Berkeley, California 94720

and

Materials and Molecular Research Division
Lawrence Berkeley Laboratory
Berkeley, California 94720

and

Roger H. Koch

IBM Thomas J. Watson Research Center
Yorktown Heights, New York 10598

The current-voltage characteristics of Josephson tunnel junctions shunted by a conductance with substantial self-inductance exhibit regions of stable negative resistance. At certain values of bias current, the junctions exhibit chaos, which is manifested as a low frequency voltage noise equivalent to a noise temperature of about 10^3K. At other bias points, switching between subharmonic modes or between a subharmonic mode and a chaotic regime produces low frequency noise with a noise temperature often exceeding 10^6K. Analog simulations indicate that, at least under some conditions, the switching is induced by intrinsic thermal noise. The analog has also been used to show that switching induced by thermal noise is responsible for the noise rise observed experimentally in three-photon Josephson parametric amplifiers.

1. INTRODUCTION

There has recently been considerable interest in nonlinear systems that exhibit chaos.(1) Such systems are governed by deterministic equations, but for an appropriate choice of parameters the solutions appear to fluctuate randomly, although in fact this behavior is completely determined by the equations of motion and the given set of initial conditions. An attractive system for studying chaos is provided by the Josephson (2) junction, which has well-established equations of motion so that realistic comparisons can be made between the observed behavior of real junctions and the predictions of analog or digital simulations. Huberman, Crutchfield, and Packard (3) were the first to point out that a resistively shunted Josephson junction with appropriate parameters should exhibit chaos when driven by an external radio frequency field. This problem has been studied in detail by Kautz (4) and D'Humieres et al.(5) using computer simulations; as emphasized by D'Humieres et al.,(5) this problem is equivalent to the forced pendulum. Apart from the inherent interest in the chaotic behavior of these systems, these ideas may by very relevant to the design of devices involving the Josephson effect. For example, it has been suggested that the large levels of excess noise observed in Josephson parametric amplifiers (6-16) were due to chaos, although there is hardly widespread agreement on this point.(13-16) Unfortunately, there has been relatively little experimental work on chaos in Josephson junctions under conditions where the experimental parameters are sufficiently well known that one can make meaningful comparisons with theoretical predictions; in particular it is very difficult to estimate the magnitude of the rf voltage across the junction. Because of this problem, we have chosen to study chaotic effects in a different system, namely a Josephson tunnel junction with self-capacitance that is shunted by a resistance with substantial self-inductance.(17)

We first describe the model system, and obtain the equations of motion. We next describe the junction configurations used, outline the measurement techniques, and present the experimental data. We discuss solutions to the equations of motion obtained on an analog computer, and show that all the features observed experimentally can be explained with the analog. We find from simulations that there are period-doubling sequences to chaos, followed by intermittency and odd- and even-period windows. In addition, we find large amounts of low frequency noise arising from switching induced by thermal noise between stable subharmonic modes or between a stable mode and a chaotic regime. As an example of the importance of these switching processes

in a practical device, we describe the results of an analog simulation of a three-photon parametric amplifier. We conclude with a brief summary.

2. EQUATIONS OF MOTION

The Josephson junction that we have investigated is shown schematically in Fig. 1. The junction

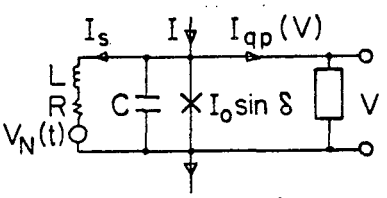

Figure 1 : Schematic representation of a Josephson tunnel junction with critical current I_o and self-capacitance C shunted with an external resistance R which has a self-inductance L. The junction is also shunted with the quasiparticle tunneling conductance, $1/R_J$.

has a critical current I_o and is shunted by its self-capacitance, C, and the quasiparticle tunneling conductance, $1/R_J$, through which the quasiparticle current I_{qp} flows. The external shunt has a resistance R and a self-inductance L, through which a current I_s flows; the resistance R generates a Nyquist voltage noise, $V_N(t)$, with a spectral density

$$S_v(f) = 4k_BTR, \tag{1}$$

where T is the temperature and f is the frequency. The coupled equations of motion can be written in the form

$$I = I_o\sin\delta + \hbar C\ddot{\delta}/2e + I_s + I_{qp}, \tag{2}$$

and

$$\hbar\dot{\delta}/2e = I_sR + \dot{I}_sL + V_N(t). \tag{3}$$

Here, I is the fixed bias current, δ is the phase difference across the junction, and we have set $\dot{\delta} = 2eV/\hbar$, where the dot implies the differentiation with respect to time. It is convenient to rewrite these equations in a dimensionless form by introducing a dimensionless time variable $t/(\Phi_o/2\pi I_oR)$, where $\Phi_o \equiv h/2e$ is the flux quantum. We obtain

$$i = \sin\delta + \beta_C\ddot{\delta} + i_s + i_{qp}, \tag{4}$$

and

$$\dot{\delta} = i_s + \beta_L\dot{i}_s + v_N. \tag{5}$$

In these equations, we have set $i = I/I_o$, $i_s = I_s/I_o$, $i_{qp} = I_{qp}/I_o$, $v_N = V_N/I_oR$, $\beta_C = 2\pi I_oR^2C/\Phi_o$, $\beta_L = 2\pi LI_o/\Phi_o$, and $\Gamma = 2\pi k_BT/I_o\Phi_o$. The three parameters that determine the behavior of the system are β_L (the reduced inductance), β_C (the reduced capacitance), and i (the reduced bias current); for a given junction i serves as the control parameter.

3. EXPERIMENTAL TECHNIQUES

We have studied two types of junction, illustrated in Fig. 2. The small area junctions (10×10 μm^2), shown in Fig. 2(a), were fabricated in

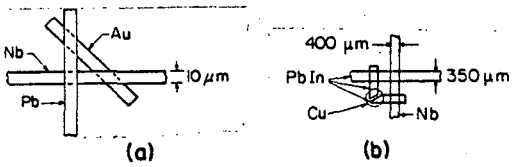

Figure 2 : (a) Small and (b) large area Josephson tunnel junctions shunted by an external resistance with substantial self-inductance. In (b), the loop is overlaid with a superconducting ground plane, insulated from the loop with a layer of SiO.

nine batches of six junctions on a 50 mm diameter Si wafer, using photolithographic lift-off techniques. First, a gold strip about 10 μm wide and 160 nm thick was deposited, followed by a Nb strip about 200 nm thick. The lift-off for the Nb strip was performed, and the resist patterned for the PbIn (5 wt.%In) strip. The wafer was diced to give nine individual substrates, each with six junctions; each substrate was processed individually from this point. The surface of the Nb was cleaned by ion-milling in Ar, and oxidized with a radio frequency discharge in an Ar-O_2 mixture. The PbIn film, about 300 nm thick, was then deposited and lifted off. Typical parameters for these junctions were I_o = 0.5 mA, C = 4 pF, R = 0.4 Ω, and L = 4 pH. The large area junctions (400×350 μm^2), shown in Fig. 2(b), were fabricated by depositing films through metal shadow masks. First, a disk of Cu about 300 nm thick was deposited, followed by two strips of PbIn that overlap the Cu. A Nb strip about 400 μm wide and 300 nm thick was sputtered and oxidized thermally. The junction was completed by depositing a 170 nm-thick PbIn strip. The sample was covered with an insulating SiO layer about 130 nm thick, and a PbIn ground plane was evaporated to reduce the inductance of the loop. Typical parameters were I_o = 1 mA, C = 6 nF, R = 2 mΩ, and L = 3 pH.

Several different measurements were made. First, we obtained a current voltage (I-V) characteristic by slowly sweeping the current, and recording the resulting voltage. Second, we measured the low frequency voltage noise across the junction by amplifying the noise with a cooled resonant tank circiut, with a resonant frequency, f_t, of about 100 kHz, coupled via a room temperature preamplifier to a mean square voltmeter. For the large area junctions, the bandwidth, B, of the measurement was determined by the Q ($\approx$ 480) of the tank circuit: $B = \pi f_T/2Q$. For the small area junctions, a lower Q ($\approx$ 60) was used, and the bandwidth was limited by a low pass fil-

ter in the subsequent signal processing to about 250 Hz. Third, in the case of the large area junctions, we connected the junctions directly to a low noise high frequency preamplifier, with a bandwidth of about 1 GHz, and examined the voltage on a spectrum analyzer.

4. EXPERIMENTAL RESULTS

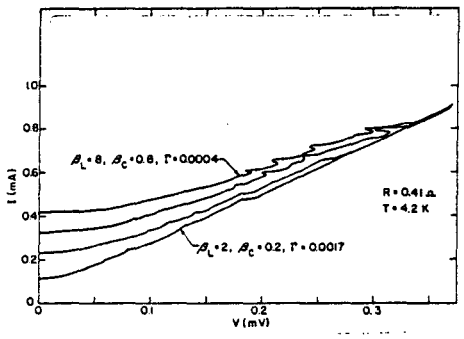

Figure 3 : Current-voltage (I-V) characteristics of a small area junction for four values of critical current.

Figure 3 shows the I-V characteristic of a small area junction for four values of critical current; the critical current was reduced by trapping magnetic flux in the junction. The characteristics of the two higher values of critical current exhibit stable regions of negative dynamic resistance. The I-V characteristics of the two lower values of critical current show structure on the I-V characteristics, but the dynamic resistance is always positive.

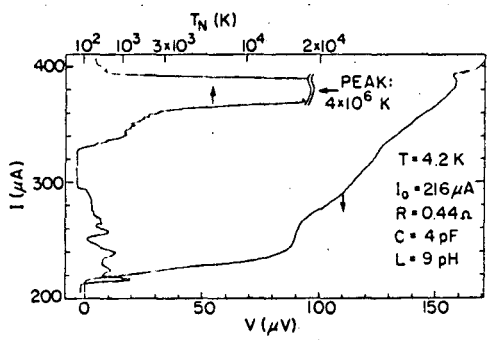

Figure 4 : I-V characteristic and voltage noise temperature, T_N, at 97 kHz for a small area junction with $\beta_C = 0.5$, $\beta_L = 6$, and $\Gamma = 8.1 \times 10^{-4}$. T_N was measured at a reduced frequency of 2.1×10^{-6}.

Figure 4 shows the I-V characteristic of a different small area junction, and, in addition, the voltage noise measured at a frequency of 97 kHz with a tank circuit Q of 57. This frequency corresponds to a reduced frequency of 2.1×10^{-6} in units of the characteristic frequency $I_o R/\Phi_o$. The noise has been characterized by a noise temperature, T_N, defined by

$$T_N = \langle V_N^2 \rangle / 4k_B RB, \qquad (6)$$

where $\langle V_N^2 \rangle$ is the mean square voltage across the junction. The noise temperature, T_N, as a function of bias current generally falls into one of three ranges. An example of the first occurs for the bias region near 300 μA. Here the noise is independent of bias current, with a magnitude of about 40K. This noise arises from the preamplifier and from Nyquist noise associated with losses in the tank circuit rather than from the junction itself. The second range of noise level appears, from example, in the intervals from 220 to 295 μA and 330 to 360 μA. Here we observe noise temperatures varying from several hundred to one thousand Kelvin. Finally, there is an enormous peak that is off-scale on this plot. In a separate measurement we found that its noise temperature was about 4×10^6K. This peak occurs just below the negative resistance region on the I-V characteristic.

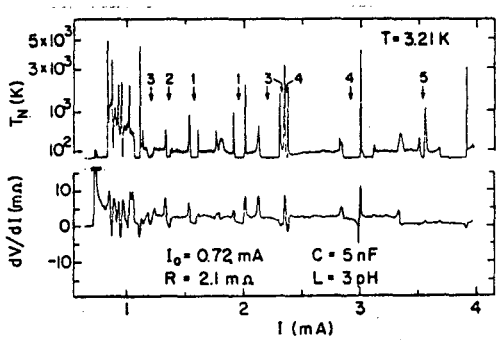

Figure 5 : dV/dI vs. I and T_N vs. I for large area junction with $\beta_C = 0.05$, $\beta_L = 6.6$, and $\Gamma = 1.9 \times 10^{-4}$. The numbers on the upper trace refer to the subharmonic number. T_N was measured at a reduced frequency of 1.6×10^{-4}.

Figure 5 shows the dynamic resistance, dV/dI, vs. I and T_N vs. I for a large area junction. There is considerable structure, including numerous values of current for which the dynamic resistance is negative. The noise temperature again shows three types of regions: Regions of about 32K, where the noise arises from the tank circuit and the preamplifier, broad regions of a hundred Kelvin, and large spikes where the noise is several thousand Kelvin. These spikes are sometimes but by no means always associated with local maxima in the dynamic resistance. Several of the regions where the noise is low have been labelled with the subharmonic number of the oscillations. This number was obtained by amplifying the signal across the junction

with the wideband amplifier, determining the fundamental frequency on a spectrum analyzer, and dividing this frequency into the Josephson frequency 2eV/h. It is evident that both even and odd subharmonics are present.

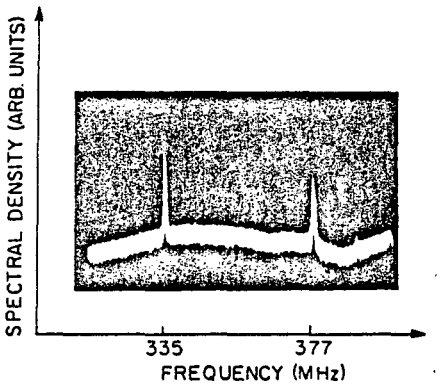

Figure 6 : Power spectrum of voltage across a large area junction at 4.2K with I_o = 2.35 mA, I = 6.68 mA, C = 5 nF, R = 1.7 mΩ, L = 3 pH, β_C = 0.10, β_L = 21, and $\Gamma = 7.5 \times 10^{-5}$.

Finally, we examined the voltage across a large area junction when it was biased at a low frequency noise spike, and displayed the result on a spectrum analyzer. The result of such a measurement is shown in Fig. 6, where we observe two well-defined peaks at 335 MHz and 377 MHz. As one sweeps the bias current through the region where the noise spike occurs, one observes first one peak, then the growth of the second peak as the first one shrinks, and finally the disappearance of the first peak. Thus, the junction switches between two subharmonic modes, giving rise to large levels of noise at frequencies below the characteristic switching frequencies. Switching between a subharmonic mode and a chaotic regime can also occur (see below): A manifestation of this behavior is the appearance of a low frequency noise spike at the boundary between noise free and moderately noisy regions. Examples of this appear in Fig. 5 at about 1.11 mA and 2.02 mA.

In order to shed more light on the behavior observed experimentally, we have performed extensive digital and analog simulations. Some of the results of the analog simulation are now briefly reported.

5. ANALOG SIMULATIONS

We have simulated the junction using an electronic analog of a Josephson junction involving a phase-locked loop (Philipp Gillette and Associates, model JA-100). To achieve large inductances (1 - 10H) with low loss, we used an active circuit for the inductance of the shunt.

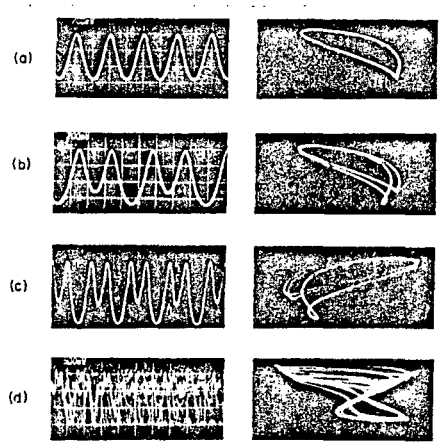

Figure 7 : Voltage vs. time (left-hand column) and $\dot{\delta}$ vs. sinδ (right-hand column) for the analog simulator with β_C = 0.25, β_L = 8.0, and $\Gamma \approx 0$: (a) period 1, (b) period 2, (c) period 4, and (d) chaos.

In Fig. 7 we show a typical set of solutions for β_C = 0.25, and β_L = 8.0. The left-hand column shows the voltage across the junction vs. time for four values of bias current, while the right-hand column shows the corresponding phase portrait, $\dot{\delta}$ vs. sinδ. In (a), the solution is the Josephson oscillation with period 1, and the corresponding phase portrait is a single closed loop that repeats each time δ evolves through 2π. In (b), a bifurcation has occurred to a period 2 solution, and the phase portrait contains two loops. In (c), a second bifurcation has occurred to a period 4 solution, while in (d) the system has become chaotic. This is an illustration of a Feigenbaum (18) period-doubling sequence to chaos.

As the current is further reduced, the system exhibits Pomeau-Manneville (19) intermittency, followed by tangent bifurcations to limit cycles of even or odd periodicity. In the theory of chaotic behavior for one-dimensional mappings with single quadratic maxima, there is an explicit sequence in which stable limit cycles of period n should first appear as the control parameter is varied monotonically.(20) The behavior we observe in our junctions as the bias current is reduced does not appear to fit this simple picture, suggesting that a reduction of this third-order system to a one-dimensional mapping may not be possible. The lack of order in the appearance of periodic windows also indicates that the basins of attraction are probably quite complicated, and that the observed behavior may depend crucially on the amount of external noise present.

In Figs. 8 and 9 we show two current-voltage characteristics obtained from the simulator with

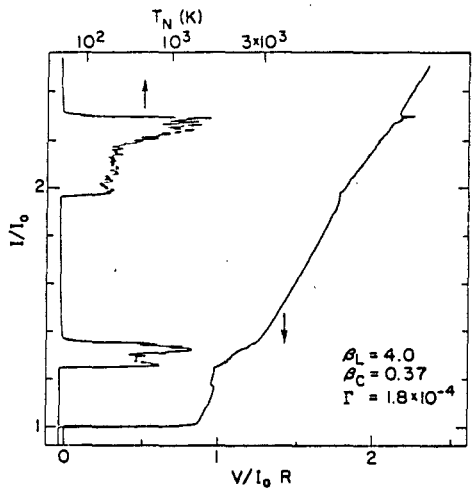

Figure 8 : I/I_o vs. V/I_oR and T_N vs. I/I_o for analog simulator with parameters chosen to approximate those of the junction in Fig. 4. T_N was measured in the reduced frequency range 0.016 to 0.079.

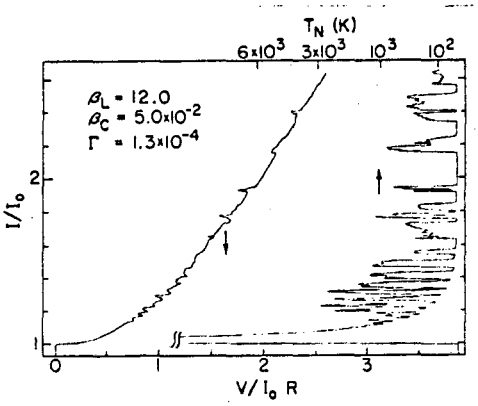

Figure 9 : I/I_o vs. V/I_o R and T_N vs. I/I_o for analog simulator with parameters chosen to approximate those of the junction in Fig. 5. T_N was measured in the reduced frequency range 0.016 to 0.079.

values of β_C, β_L, and Γ chosen to approximate those of the real junctions in Figs. 4 and 5. We observe the same general structure on the characteristics, including regions of stable negative resistance. Also shown in Figs. 8 and 9 are the corresponding noise temperatures, measured at frequencies between 10 and 50 Hz, corresponding to reduced frequencies of 0.016 and 0.079. In the region of low noise, the junction is in a stable limit cycle, and the noise is from the measurement system. There are also relatively broad regions of current where the noise ranges from a few hundred Kelvin to perhaps 10^3K: In these regions the junction is chaotic. Thus, for the experimental junctions, we can identify the values of bias current where the noise is of the same order of magnitude as regions in which chaos occurs.

Notice that the very large noise temperatures ($\gtrsim 10^5$K) measured in the real junctions are not present in the bandwidth of the noise measurements in Figs. 8 and 9. For the real junctions, the noise measurements in Figs. 4 and 5 were performed at reduced frequencies, $f/(I_oR/\Phi_o)$, of 2.1×10^{-6} and 1.6×10^{-4}, respectively, while for the simulations the reduced frequency of the measurements spans the range 0.016 to 0.079. The lack of a large noise peak in this portion of the analog spectrum suggests than switching noise is greater at much lower reduced frequencies.

In order to observe this switching behavior on the analog, we measured the power spectrum of the noise down to dimensionless frequencies equivalent to those of the measurements on the large-area junctions. In Fig. 10, we show the spectral density of the voltage noise at a bias

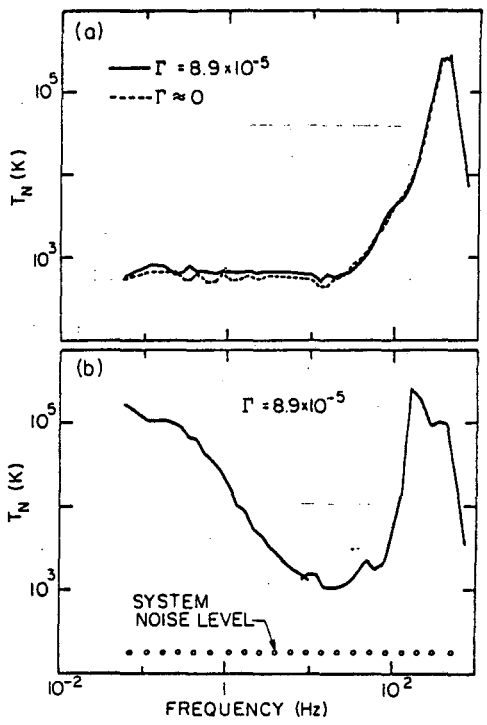

Figure 10 : Noise temperature (for I_o = 1.49 mA) for analog with β_C = 0.105 and β_L = 12.0 (a) in chaotic regime and (b) in switching regime, with and without thermal noise. The horizontal scale spans the normalized frequency range 1.55×10^{-5} to 1.55.

point where the system is chaotic, and at a point where switching occurs between a subharmonic mode and a chaotic regime. In the chaotic regime, we see a residual, broadened subharmonic peak at about 500 Hz, and at lower frequencies white noise with a noise temperature of about 700K. We notice that this behavior is essentially independent of the presence or absence of injected thermal noise equivalent to 3.18K. In the absence of injected noise, the intrinsic noise temperature of the analog was $\lesssim 7$ mK. In Fig. 10(b), the noise temperature of the junction in the absence of thermal noise is below the noise temperature of the measurement system. In the presence of thermal noise equivalent to 3.18K, however, the noise temperature increases dramatically, with a power spectrum of approximately 1/f at frequencies below 10 Hz to a value of about 10^5K at 0.1 Hz. The 1/f nature of this noise has also been observed in real junctions. Thus, it appears that this type of behavior is due to thermal noise currents that can induce the system to "hop" between two different regimes, for example, two subharmonic modes that would be stable in the absence of thermal noise, or between a subharmonic mode and a chaotic region. Somewhat related behavior has been discussed by Arrecchi and Lisi (21) for a non-linear electronic oscillator. However, these authors claim that the 1/f noise is intrinsic to the deterministic equation of motion, without the addition of thermal noise. Hopping between modes has also been discussed by Kautz,(4) D'Humieres et al.,(5) and Ben-Jacob et al.,(22) but they do not appear to have observed a 1/f power spectrum.

6. JOSEPHSON PARAMETRIC AMPLIFIERS

To illustrate the importance of some of the ideas described above to practical devices, we consider briefly the Josephson parametric amplifier. The inductance of a Josephson junction for $I < I_o$ is non-linear, and may be written in the form (2)

$$L_J = \Phi_o/2\pi I_o \cos\delta = \Phi_o/2\pi(I_o^2 - I^2)^{\frac{1}{2}}. \qquad (7)$$

This non-linearity may be used for parametric amplification of electromagnetic signals, and amplifiers of this kind have been extensively studied. There are two principal modes of operation, the singly-degenerate three-photon mode, (9-12) and the doubly-degenerate four-photon mode.(6-8) We shall confine ourselves to the former, in which the pump frequency, ω_p, the signal frequency, ω_s, and the idler frequency, ω_i, satisfy the relation

$$\omega_p = \omega_s + \omega_i, \qquad (8)$$

where $\omega_s \approx \omega_i \approx \omega_p/2$. The junction is biased with a current below the critical current, and an appropriate level of pump power is applied. Both the bias current and pump amplitude change the plasma frequency of the junction according to the relation

$$\omega_o(n, I/I_o) = \omega_o(0,0)[J_o(n)]^{\frac{1}{2}}[1 - (I/I_o)^2]^{\frac{1}{4}}, \qquad (9)$$

where

$$n = 2\pi V_p/\Phi_o\omega_p. \qquad (10)$$

Here,

$$\omega_o(0,0) = (I_o/2\pi\Phi_o C)^{\frac{1}{2}} \qquad (11)$$

is the maximum plasma frequency, and V_p is the voltage across the junction at the pump frequency. Thus, one adjusts the bias current and pump amplitude until the plasma frequency is equal to the signal frequency. As the pump power is increased, the signal amplification increases, but, unfortunately one finds that the input noise temperature also increases. This so-called "noise rise" has prevented the Josephson parametric amplifier from becoming important as a high frequency amplifier. There have been several attempts to explain the noise rise,(13-16) but, to our knowledge, none of these explanations has been in satisfactory agreement with the observed phenomena.

We (23) have simulated the three-photon Josephson parametric amplifier using the circuit (16) shown in Fig. 11. The junction has capacitance

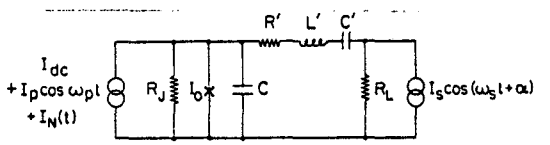

Figure 11 : Circuit for analog simulation of three-photon Josephson parametric amplifier.

C and is shunted with a resistance R_J representing the quasiparticle tunneling resistance; associated with this resistance is a Nyquist noise current, $I_N(t)$. In practice, the signal is coupled in by means of a circulator, which we represent by a series resonant circuit with inductance L', capacitance C', and resistance R'. The resistance of the signal source is R_L. The values of L' and C' were chosen so that $\omega_s = (L'C')^{-\frac{1}{2}}$. To optimize the performance, we set $R_L = R'$ and maintained $R_L + R' \approx R_J$. The Q of the resonant circuit, $(L'/C')^{\frac{1}{2}}/(R' + R_L)$ was typically 20. The pump was represented by a current source, $I_p\cos\omega_p t$. To establish parametric amplification, we first applied low levels of pump and signal power and adjusted I_{dc} until signal gain and the idler were observed. We then increased the pump amplitude, adjusting I_{dc} to achieve maximum gain.

Figure 12 shows typical results for four levels of pump power with $I_{dc}/I_o = 0.74$ and $\Gamma = 2.32 \times 10^{-5}$; this value of Γ corresponds to a temperature of 0.55K for a junction with $I_o = 1$ mA. The frequency has been normalized to $\omega_o(0,0)$. The lowest trace is for $I_p/I_o = 0$, so that a re-

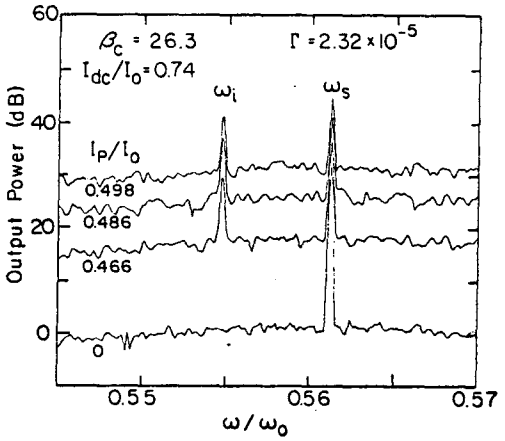

Figure 12 : Power spectral density of voltage across R_L for 4 values of I_p/I_o. Reference level of power is arbitrary. Frequency ω has been normalized to the maximum plasma frequency $\omega_o(0,0)$.

sponse is seen only at the signal frequency, ω_s. The remaining three traces show the results for increasing levels of I_p/I_o, the largest level corresponding to the maximum gain that could be achieved with the given circuit parameters. For larger values of I_p or I_{dc}, a bifurcation occurs to an oscillation at $\omega_p/2$. This behavior, which is also seen in real devices, (24) is a useful means of recognizing that the condition for maximum gain has been achieved. Once the bifurcation has occurred, the gain drops sharply. We see in Fig. 12 that while the signal gain increases as the pump power increases, the level of the noise increases much more dramatically. Thus, when the pump power is increased from zero to its value for maximum gain, the signal gain is 12.8 dB, while the noise increases by 30 dB. To illustrate the much more rapid rise in noise than in signal gain, in Table I we have listed the signal gain, G_S, the noise gain, G_N, and their ratio G_N/G_S for 4 values of I_p/I_o. The gains G_S and G_N (measured at frequency ω_s) are the ratios of the signal and noise powers, respectively, to their values at $I_p/I_o = 0$. Notice that G_N/G_S, which is proportional to the noise temperature T_N, increases from 12 dB to 17 dB as the signal gain is increased from 4.7 dB to 12.8 dB. (By way of comparison, for an amplifier with no noise rise we would have G_N/G_S = 1, independent of G_S.) The observed noise rise is such that G_N/G_S, and hence T_N, rise faster than G_S for low values of G_S. This result is consistent with data obtained by Mygind et al. (10) for a real amplifier when they varied the applied pump power.

Table I : Signal gain, G_S, at $\omega = \omega_s$, noise gain, G_N, for $\omega \approx \omega_s$, and G_N/G_S for the amplifier represented in Fig. 12.

I_p/I_o	Signal Gain G_S (dB)	Noise Gain G_N (dB)	G_N/G_S (dB)
0.466	4.7 ± 0.1	16.7 ± 0.4	12.0 ± 0.4
0.475	6.9 ± 0.1	17.7 ± 0.4	10.8 ± 0.4
0.486	9.3 ± 0.1	24.9 ± 0.7	15.6 ± 0.7
0.498	12.8 ± 0.1	30.0 ± 0.4	17.2 ± 0.4

We have also performed simulations for $\Gamma \approx 6.1 \times 10^{-7}$. In this limit, substantial amounts of signal gain were achieved, without an accompanying noise rise. However, other simulations suggest that the threshold level of the thermal noise is quite low: We observed a noise rise for $\Gamma = 4.2 \times 10^{-6}$ corresponding to a temperature of 0.1K for a junction with I_o = 1 mA.

From these results, we can draw two important conclusions concerning noise in the three-photon parametric amplifier. First, the noise cannot arise from chaos: To achieve gain, one always operates the amplifier with I_{dc} and I_p below the threshold for a period-doubling bifurcation of the pump frequency. Second, the observed noise rise requires the presence of thermal noise. We believe the noise rise is due to hopping between a bias point in the high gain region (that would be stable in the absence of thermal noise) and an unstable point in the bifurcated region. Since an increase in gain necessarily implies that the device is closer to the bifurcation threshold, one would expect that the probability of hopping and hence the noise produced would increase as the gain is increased.

Finally, we emphasize that the amplification process in the four-photon Josephson parametric amplifier is quite different from that just described, and the device is not operated near a period-doubling bifurcation. Thus, we believe that the mechanism we have described here does not account for the noise in the four-photon amplifier.

7. SUMMARY

We have described the properties of Josephson tunnel junctions shunted by a resistance with non-negligible self-inductance and biased with a constant current. The general features observed for the experimental junctions are explained very adequately by analog simulations. The I-V characteristics usually exhibit regions of stable negative resistance that can be reduced in extent and made to disappear by the progressive reduction of the critical current in an external magnetic field. When the junction is in a stable limit cycle, which may or may not be bifurcated, the voltage noise is below the level of the measurement system. In the chaotic regimes, the noise temperature of the junction is typically a few hundred Kelvin. At certain values of the bias current the noise temperatures may become very large, often exceeding 10^6K. These noise temperatures, which increase as the measurement frequency is de-

creased, arise from switching between two subharmonic modes or between a subharmonic mode and a chaotic regime. The analog simulations indicate that, at least under certain conditions, this switching is induced by relatively low levels of intrinsic thermal noise; in the absence of thermal noise, the switching did not occur. However, we would not rule out other situations in which the switching is intrinsic to the equations of motion, and is not induced by thermal noise.

As an example of the importance of the switching mechanism, we have used the analog simulator to study noise in the three-photon Josephson parametric amplifier. The amplifier gain increases as the pump amplitude is increased until the system is about to bifurcate to the half-harmonic of the pump frequency. At that point, the gain drops dramatically. The simulations show no noise rise in the absence of thermal noise. However, a small level of thermal noise is sufficient to produce a dramatic increase in the noise in the amplifier. We believe that this noise rise is produced by switching between bias points in the bifurcated and unbifurcated regions.

ACKNOWLEDGMENTS

We are indebted to Henry Abarbanel, Raymond Chiao, John David Crawford, Bernardo Huberman, Edgar Knobloch and Kurt Wiesenfeld for very helpful discussions. T. D. Van Duzer kindly lent us the analog simulator. We are indebted to the Micro Electronics Facility in the Electronics Research Laboratory of the Electrical Engineering and Computer Science Department of the University of California at Berkeley for the use of their facilities. This work was supported by the Director, Office of Basic Energy Sciences, Materials Sciences Division of the U. S. Department of Energy under Contract Number DE-AC03-76SF00098.

REFERENCES

[1] For reviews, see, for example, May, R.M., Simple mathematical models with very complicated dynamics, Nature 261 (1976) 459-467; Eckmann, J.-P., Roads to turbulence in dissipative dynamical systems, Rev. Mod. Phys. 53 (1981) 643-654.

[2] Josephson, B.D., Possible new effects in superconductive tunneling, Phys. Lett. 1 (1962) 251-253; Supercurrents through barriers, Adv. in Phys. 14 (1965) 419-451.

[3] Huberman, B.A., Crutchfield, J.P., and Packard, N.H., Noise phenomena in Josephson junctions, Appl. Phys. Lett. 37 (1980) 750-752.

[4] Kautz, R.L., The ac Josephson effect in hysteretic junctions: Range and stability of phase lock, J. Appl. Phys. 52 (1981) 3528-3541; Chaotic states of rf-biased Josephson junctions, J. Appl. Phys. 52 (1981) 6241-6246; Chaos in Josephson circuits, IEEE Trans. Mag. (1983) to be published.

[5] D'Humieres, D., Beasley, M.R., Huberman, B. A., and Libchaber, A., Chaotic states and routes to chaos in the forced pendulum, Phys. Rev. A 26 (1982) 3483-3496.

[6] Feldman, M.J., Parrish, P.T., and Chiao, R. Y., Parametric amplification by unbiased Josephson junctions, J. Appl. Phys. 46 (1975) 4031-4042.

[7] Taur, Y. and Richards, P.L., Parametric amplification and oscillation at 36 GHz using a point contact Josephson junction, J. Appl. Phys. 48 (1977) 1321-1326.

[8] Wahlsten, S., Rudner, S., and Claeson, T., Arrays of Josephson tunnel junctions as parametric amplifiers, J. Appl. Phys. 49 (1978) 4248-4263.

[9] Mygind, J., Pedersen, N.F., and Soerensen, O.H., X-band singly degenerate parametric amplification in a Josephson tunnel junction, Appl. Phys. Lett. 32 (1978) 70-72.

[10] Mygind, J., Pedersen, N.F., Soerensen, O.H., Dueholm, B., and Levinsen, M.T., Low-noise parametric amplification at 35 GHz in a single Josephson tunnel junction, Appl. Phys. Lett. 35 (1979) 91-93.

[11] Levinsen, M.T., Pedersen, N.F., Soerensen, O.H., Dueholm, B., and Mygind, J., Externally pumped millimeter-wave Josephson junction parametric amplifier, IEEE Trans. Elec. Dev. ED-27 (1980) 1928-1934.

[12] Soerensen, O.H., Dueholm, B., Mygind, J., and Pedersen, N.F., Theory of the singly quasidegenerate Josephson junction parametric amplifier, J. App.. Phys. 51 (1980) 5483-5494.

[13] Chiao, R.Y., Feldman, M.J., Peterson, D.W., Tucker, B.A., and Levinsen, M.T., Phase instability noise in Josephson junctions, in Future Trends in Superconductive Electronics, A.I.P. Conf. Proc. 44 (1978) 259-263.

[14] Feldman, M.J. and Levinsen, M.T., Theories of the noise rise in Josephson PARAMPS, IEEE Trans. Magn. MAG-17 (1981) 834-837.

[15] Pedersen, N.F. and Davidson, A., Chaos and noise rise in Josephson junctions, Appl. Phys. Lett. 39 (1981) 830-832.

[16] Levinsen, M.T., Even and odd subharmonic frequencies and chaos in Josephson junctions: Impact on parametric amplifiers?, J. Appl. Phys. 53 (1982) 4294-4299.

[17] Miracky, R.F., Clarke, J., and Koch, R.H., Chaotic noise observed in a resistively

shunted self-resonant Josephson tunnel junction, Phys. Rev. Lett 50 (1983) 856-859.

[18] Feigenbaum, M.J., Quantitative universality for a class of nonlinear transformations, J. Stat. Phys. 19 (1978) 25-52; The universal metric properties of nonlinear transformations, J. Stat. Phys. 21 (1979) 669-706.

[19] Manneville, P. and Pomeau, Y., Intermittency and the Lorenz model, Phys. Lett. 75A (1979) 1-2; Pomeau, Y. and Manneville, P., Intermittent transition to turbulence in dissipative dynamical systems, Commun. Math. Phys. 74 (1980) 189-197.

[20] Metropolis, N., Stein, M.L., and Stein, P. R., On finite limit sets for transformations on the unit interval, J. Combinatorial Theory 15A (1973) 25-44.

[21] Arecchi, F.T. and Lisi, F., Hopping mechanism generating 1/f noise in nonlinear systems, Phys. Rev. Lett. 49 (1982) 94-98.

[22] Ben-Jacob, E., Goldhirsch, I., Imry, Y., and Fishman, S., Intermittent chaos in Josephson junctions, Phys. Rev. Lett. 49 (1982) 1599-1602.

[23] Miracky, R.F. and Clarke, J., Simulation of the noise rise in three-photon Josephson parametric amplifiers, (1983) submitted to Appl. Phys. Lett.

[24] Pedersen, N.F., Soerensen, O.H., Dueholm, B., and Mygind, J., Half-harmonic parametric oscillations in Josephson junctions, J. Low Temp. Phys. 38 (1980) 1-23.

TECHNICAL INFORMATION DEPARTMENT
LAWRENCE BERKELEY LABORATORY
UNIVERSITY OF CALIFORNIA
BERKELEY, CALIFORNIA 94720